Photoluminescence of $RbCaF_3:Mn^{2+}$: the influence of phase transitions

1993 J. Phys.: Condens. Matter 5 1437

(http://iopscience.iop.org/0953-8984/5/9/028)

J. Phys.: Condens. Matter 5 (1993) 1437–1446. Printed in the UK

Photoluminescence of $RbCaF_3:Mn^{2+}$: the influence of phase transitions

M C Marco de Lucas, F Rodríguez and M Moreno

DCITTYM (Sección Ciencia de Materiales), Facultad de Ciencias, Universidad de Cantabria, 39005-Santander, Spain

Received 19 October 1992, in final form 7 December 1992

Abstract. Precise photoluminescence measurements on an $RbCaF_3:Mn^{2+}$ sample containing *only* 400 ppm of Mn^{2+} have been carried out in the 10–300 K temperature range. The results are compared with those obtained in other fluoroperovskites doped with Mn^{2+}. The analysis of the $^6A_{1g}(S) \rightarrow {}^4T_{1g}(G)$ excitation peak at room temperature leads to a Mn^{2+}–F^- distance $R = 213.3$ pm which is close to that derived from the experimental isotropic superhyperfine constant, A_s. The plot of the first moment of the emission band, M_1, against temperature reveals a slight but sensible change of slope at $T = 193$ K which is associated with the $O_h^1 \rightarrow D_{4h}^{18}$ structural phase transition of the host lattice. Furthermore, at $T = 40$ K, M_1 undergoes an abrupt increase of ~ 100 cm^{-1}. This fact supports the existence of *another* phase transition involving an increase $\Delta R/R \simeq 0.2\%$ upon cooling, and thus a situation which is similar to that detected in the structural phase transition of $KMnF_3$ at $T_c = 81.5$ K. To our knowledge this is the first time that clear evidence of both phase transitions in $RbCaF_3$ has been achieved through an optical probe. Finally the variation of the $^4A_{1g}(G)$, $^4E_g(G)$ peak, E_3, along the fluoroperovskite series is analysed.

1. Introduction

Some cubic fluorides doped with Mn^{2+} are among the few systems where a local structural characterization around the impurity has properly been achieved. As an example the Mn^{2+}–F^- distance, R, between the substitutional Mn^{2+} impurity and the nearest F^- ions has been determined for $KZnF_3:Mn^{2+}$ and $RbCdF_3:Mn^{2+}$ using three independent methods: (1) the extended x-ray absorption fine structure (EXAFS) technique [1]; (2) the analysis of the isotropic superhyperfine (SHF) constant, A_s [2, 3]; and (3) the analysis of excitation spectra obtained through photoluminescence [4, 5]. In this line very recent EXAFS measurements on $CaF_2:Mn^{2+}$ lead to $R = 227$ pm [6] which is coincident with previous determinations from the experimental A_S value [3].

As a common feature for isolated Mn^{2+} in cubic fluorides it has been demonstrated that crystal-field spectra and electron paramagnetic resonance (EPR) parameters can reasonably be understood only on the basis of *isolated* MnF_N units whose equilibrium distance, R, is influenced by the chemical pressure exerted by the rest of the lattice. In the series of cubic fluoroperovskites (at room temperature) such a pressure orders the R values as the corresponding values, R_0, for the perfect lattice although the two figures are usually different for a given lattice. This situation is reviewed in [7].

0953-8984/93/091437+10$07.50

Although a great many cubic fluoroperovskites doped with Mn^{2+} have been investigated through EPR [8] (and some of them also by electron-nuclear double resonance (ENDOR) [9–11]) the number of such systems explored using photoluminescence techniques is certainly smaller. This is partly because of the very small oscillator strengths ($f \simeq 10^{-8}$) associated with crystal-field transitions of isolated MnF_6^{4-} units in cubic symmetry which makes it difficult to detect photoluminescence spectra when the Mn^{2+} concentration is below about 1000 ppm.

The present work is devoted to exploration of the luminescence and excitation spectra of an $RbCaF_3:Mn^{2+}$ sample containing only about 400 ppm of Mn^{2+} as well as the associated lifetime in the 10 K–300 K range. Apart from detecting the photoluminescence due to MnF_6^{4-} a first goal of our investigation is to explore whether or not the crystal-field spectrum of $RbCaF_3:Mn^{2+}$ is compatible with an Mn^{2+}–F^- distance $R = 214.2(6)$ pm as previously derived from the analysis of the experimental A_s value [2]. Other goals of the present work are related to phase transitions in $RbCaF_3$. This compound has a clearly established $O_h^1 \rightarrow D_{4h}^{18}$ structural phase transition at $T_{c1} = 193$ K [12–18]. This phase transition is also observed in $RbCdF_3$ ($T_c = 124$ K) [19] but not in $CsCaF_3$ [20]. EPR results on $RbCaF_3:Mn^{2+}$ and $RbCdF_3:Mn^{2+}$ [8, 21], and specially ENDOR data on the latter system [11] indicate that the local geometry around Mn^{2+} is practically octahedral in the tetragonal phase. To be more specific, if R_{ax} and R_{eq} denote respectively the axial and equatorial Mn^{2+}–F^- distances of the distorted MnF_6^{4-} unit in the tetragonal phase, it has been found that $R_{ax} - R_{eq} = 0.2$ pm for $RbCdF_3:Mn^{2+}$ at $T = 30$ K [7]. This value has to be compared with $R_{ax}^0 - R_{eq}^0 = 1.1$ pm corresponding to the perfect lattice [19]. A similar situation would occur for $RbCaF_3:Mn^{2+}$ as discussed in [7]. Thus if changes in the optical spectrum of Mn^{2+} in fluorides mainly reflect geometrical changes in the first coordination sphere the detection of the phase transition of $RbCaF_3$ at $T_{c1} = 193$ K using optical parameters of the Mn^{2+} impurity as probe is not in principle a simple task. Recent results by Villacampa *et al* on $RbCdF_3:Cr^{3+}$ [22] supported this view. In order to demonstrate the influence of this phase transition upon optical parameters associated with MnF_6^{4-} in $RbCaF_3:Mn^{2+}$, measurements on $CsCaF_3:Mn^{2+}$ under the same experimental conditions have also been performed.

As a last goal this work is also devoted to explore the existence of *another* phase transition in $RbCaF_3$ at $T_{c2} \cong 40$ K. Evidence of such a phase transition has been obtained through early heat capacity, dielectric and Raman studies [12, 13] as well as by subsequent x-ray and dielectric measurements by Hidaka *et al* [18]. Nevertheless no indication of this phase transition has been achieved through the neutron measurements carried out by Kamitakahara and Rotter [14]. Also other studies devoted to exploring the first phase transition at $T_{c1} = 193$ K seem to have paid no attention to the second one [15–17, 21] and so it thus deserves further investigation.

2. Experimental details

The single crystals of $RbCaF_3:Mn^{2+}$ used in this work were kindly provided by Professor R Alcalá. The actual Mn^{2+} concentration, 400 ± 100 ppm, was estimated by measuring the EPR integrated intensity at RT of a powder (obtained from the sample) and comparing it to the corresponding value for a $KZnF_3:Mn^{2+}$ powder with 2% Mn^{2+}. Qualitatively speaking the low concentration of Mn^{2+} in our $RbCaF_3$ sample

is also supported by the well resolved SHF structure seen in its EPR spectrum. That structure is however fully absent for the $KZnF_3:Mn^{2+}$ powder where the average distance between closest Mn^{2+} would be about 3.7 times smaller than in our sample. The value of the isotropic SHF constant $A_s = 14.4(4) \times 10^{-4}$ cm^{-1} measured at RT for $RbCaF_3:Mn^{2+}$ is essentially coincident with $A_s = 13.9(3) \times 10^{-4}$ cm^{-1} previously reported by Rousseau *et al* [8].

For obtaining excitation and emission spectra of $RbCaF_3:Mn^{2+}$ as well as for carrying out lifetime measurements it was necessary to improve the detection sensitivity because of the low value of the Mn^{2+} concentration.

Excitation spectra were obtained with an implemented Jobin Yvon JY-3D fluorimeter [23] equipped with a photon counting facility. The excitation beam was chopped and focused on the sample which was coupled to an Oriel interference filter ($\lambda = 600$ nm) in front of a Hamamatsu R928 photomultiplier. The luminescence signal was measured during the non-excitation periods with a Stanford System SR440 preamp and SR 400 photon counter.

Luminescence spectra were obtained by means of a Jobin Yvon HR-320 monochromator employing the chopping light of a Spectra Physics model 2020-03 Ar laser as excitation source.

For lifetime measurements, the luminescence signal was digitized by means of a Tektronix 2430A scope.

Temperature variations were achieved by a Scientific Instruments DE-202 closed-circuit cryostat allowing temperature stabilities within 0.1 K and an accuracy of 0.5 K, with an APD-K temperature controller.

3. Results and discussion

The RT luminescence of $RbCaF_3:Mn^{2+}$ together with the corresponding excitation spectrum are shown in figure 1 where spectra of $CsCaF_3:Mn^{2+}$ are also included for comparison. As in other fluorides doped with Mn^{2+} the only emission band found in $RbCaF_3:Mn^{2+}$ is assigned as the $^4T_{1g}(G) \rightarrow {}^6A_{1g}(S)$ electronic transition thus involving the *first* excited state. The assignment of excitation bands for $RbCaF_3:Mn^{2+}$ together with the position of the corresponding maxima are given in table 1. Values of the effective Racah parameters, B and C, together with that for the cubic field splitting parameter, $10Dq$, are also given.

The excitation spectrum of $RbCaF_3:Mn^{2+}$ is very similar but not identical to that of $CsCaF_3:Mn^{2+}$ as can be inferred simply by looking at figure 1. The most significant difference between both spectra lies in the position of the first $^6A_{1g}(S) \rightarrow {}^4T_{1g}(G)$ excitation peak which is found at $\lambda = 511$ nm for $RbCaF_3:Mn^{2+}$ while it appears at $\lambda = 503$ nm for $CsCaF_3:Mn^{2+}$. This result concurs with previous work on Mn^{2+} doped fluorides showing that among the observed crystal-field transitions of MnF_6^{4-} the $^6A_{1g}(S) \rightarrow {}^4T_{1g}(G)$ is the most sensitive one to a change of the host lattice [4, 5]. Microscopically this relevant fact has been explained on the following grounds:

(i) The near independence of the effective Racah parameters B and C from R observed experimentally and well supported by theoretical calculations on MnF_6^{4-} in fluoroperovskites performed for *several* values of R [24].

(ii) The $^6A_{1g}(S) \rightarrow {}^4T_{1g}(G)$ transition is the most strongly dependent upon $10Dq$ among the observed crystal-field transitions [25].

Table 1. Experimental peak energy and assignment of the crystal field bands observed in the room temperature excitation spectra of $RbCaF_3:Mn^{2+}$ and $CsCaF_3:Mn^{2+}$, together with the fitted values of the Racah parameters B and C, and the crystal field $10Dq$. Tree's ($\alpha = -65$ cm^{-1}) and seniority ($\beta = 131$ cm^{-1}) corrections were included in the fitting. σ is the standard deviation. The position of the luminescence band is also included. Units are in cm^{-1}. The errors in the peak energies and $10Dq$ values are 20 cm^{-1} and 40 cm^{-1}, respectively.

Assignment	$RbCaF_3:Mn^{2+}$	$CsCaF_3:Mn^{2+}$
$^4T_{1g}(G) \leftarrow {}^6A_{1g}(S)$	19 560	19 880
$^4T_{2g}(G)$	23 650	23 805
$^4A_{1g}(G)$, $^4E_g(G)$	25 400	25 350
$^4T_{2g}(D)$	28 450	28 500
$^4E_g(D)$	30 280	30 265
$^4T_{1g}(P)$	32 340	31 960
B	831	834
C	3158	3141
$10Dq$	7305	6890
σ	215	225
Emission: $^4T_{1g}(G) \rightarrow {}^6A_{1g}(S)$	17 920	18 350

(iii) The significant dependence of $10Dq$ upon R found experimentally [4, 5, 26] as well as by means of theoretical calculations [24, 27] on transition-metal complexes as a function of R. This dependence can be written as

$$10Dq = KR^{-n}. \tag{1}$$

Experimentally [4, 5] a value $n = 4.7$ was found for MnF_6^{4-}. The validity of these ideas is well supported by the general view on the main optical results for Mn^{2+} doped fluoroperovskites given in table 2. Judging by these the influence of the so-called explicit temperature contribution [28, 29] to the band maxima appears to be not important as regards the comparison among all Mn^{2+} doped fluoroperovskites at RT. By contrast it plays a relevant role for understanding the temperature dependence of the peak energies for a given system [29].

Table 2. Metal–ligand distance and spectroscopic parameters in the Mn^{2+} doped ABF_3 fluoroperovskite series at room temperature. R_0 is the B^{2+}–F^- distance in the host lattice. R_C is the Mn^{2+}–F^- distance determined by EXAFS in $KZnF_3:Mn^{2+}$ and $RbCdF_3:Mn^{2+}$, and through the isotropic superhyperfine constant, A_s, in $KMgF_3:Mn^{2+}$, $RbCaF_3:Mn^{2+}$, and $CsCaF_3:Mn^{2+}$. $R4_{T_{1g}}$ and R_{10Dq} denote the R values obtained through the $^4T_{1g}(G)$ peak energy and the crystal field parameter $10Dq$, respectively (see text). Peak energies and $10Dq$ are given in cm^{-1} and distances in pm.

System	R_0	$^4T_{1g}(G)$	$^4A_{1g}$, $^4E_g(G)$	Emission	$10Dq$	R_C [7]	$R4_{T_{1g}}$	R_{10Dq}
$KMgF_3:Mn^{2+}$	199.3	18 160	25 200	16 955	8432	207.0	206.0	206.8
$KZnF_3:Mn^{2+}$	202.6	18 530 [37]	25 210 [37]	17 100 [37]	8215	208.0	208.0	208.0
$KMnF_3$	209.5	18 900 [29]	25 245 [29]	—	7853	209.5	209.9	209.9
$RbMnF_3$	212.0	19 300 [29]	25 275 [29]	—	7496	212.0	211.9	212.0
$RbCdF_3:Mn^{2+}$	220.0	19 510	25 215	17 950	7264	213.0	213.0	213.4
$RbCaF_3:Mn^{2+}$	222.7	19 560	25 400	17 920	7306	214.2	213.3	213.1
$CsCaF_3:Mn^{2+}$	226.2	19 880	25 350	18 350	6890	215.5	214.9	215.8

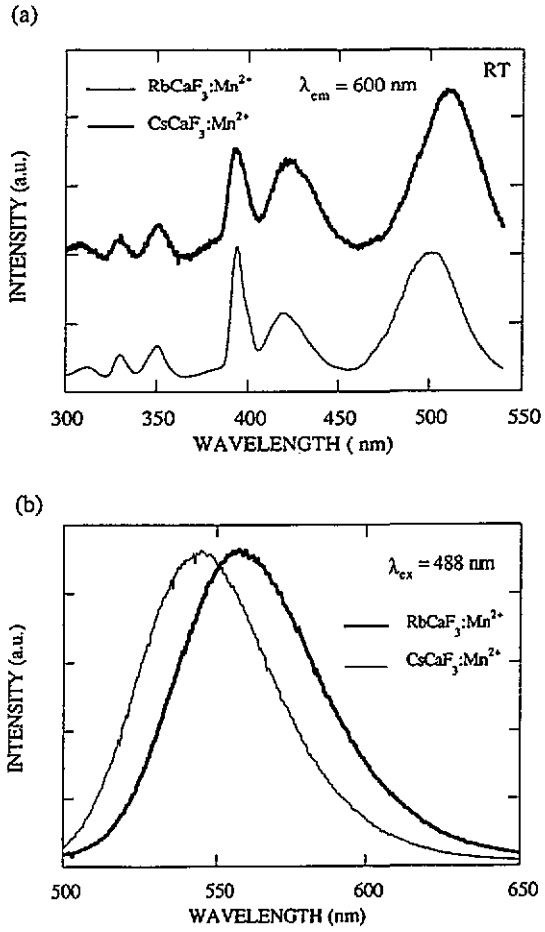

Figure 1. Room temperature (*a*) excitation and (*b*) luminescence spectra corresponding to $RbCaF_3:Mn^{2+}$ and $CsCaF_3:Mn^{2+}$. A small shoulder observed in the second excitation band peaked at $\sim$ 420 nm comes from xenon lines of the lamp.

As regards $RbCaF_3:Mn^{2+}$ itself within the series of fluoroperovskites doped with Mn^{2+} the position of the $^6A_{1g}(S) \rightarrow {}^4T_{1g}(G)$ excitation peak at RT lies between that for $RbCdF_3:Mn^{2+}$ and that for $CsCaF_3:Mn^{2+}$ as is expected provided R values along the series are *ordered* as the corresponding R_0 values. However, the small difference between the excitation peaks of $RbCdF_3:Mn^{2+}$ and $RbCaF_3:Mn^{2+}$ indicates that the corresponding R values are close to each other. This idea is also supported by the analysis of the corresponding $10Dq$ values which give rise however to an R value slightly higher for $RbCdF_3:Mn^{2+}$ than for $RbCaF_3:Mn^{2+}$.

For achieving a proper comparison between the R values of these systems we have also performed EPR measurements on a powder of $RbCdF_3:Mn^{2+}$ where the SHF structure is clearly visible. The measured value $A_s = 15.7(3) \times 10^{-4}$ cm^{-1} is higher than $A_s = 14.4(4) \times 10^{-4}$ cm^{-1} measured for $RbCaF_3:Mn^{2+}$. Such figures imply [2] that the difference, ΔR, between R values corresponding to $RbCaF_3:Mn^{2+}$ and $RbCdF_3:Mn^{2+}$ would be $\Delta R = (1.8 \pm 1.2)$ pm, and so R values would be

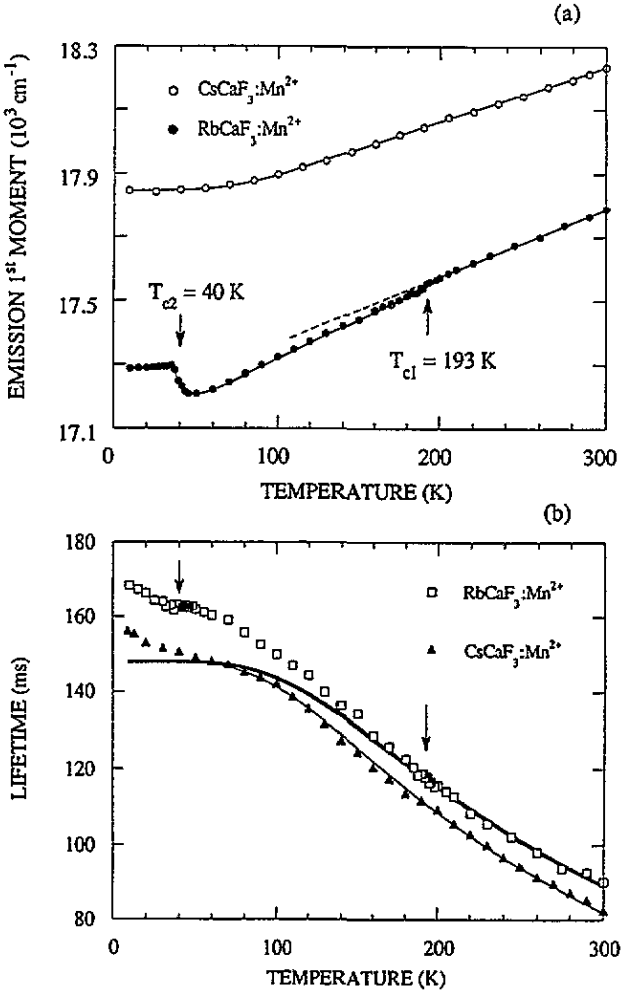

Figure 2. Plot of (*a*) the experimental luminescence first moment, M_1, and (*b*) the lifetime τ against temperature for $RbCaF_3:Mn^{2+}$ and $CsCaF_3:Mn^{2+}$. In the case of the lifetime the solid lines have been obtained through a fitting of the experimental values using equation (3). The fitted parameter values are $\hbar\omega_u = 260$ cm^{-1}, $\tau_0 = 148$ ms for $CsCaF_3:Mn^{2+}$ and $\hbar\omega_u = 290$ cm^{-1}, $\tau_0 = 148$ ms for $RbCaF_3:Mn^{2+}$. Lines in $M_1(T)$ are included as visual guides.

ordered as the corresponding R_0 values as inferred from the experimental A_s.

The main reason why the fitted $10Dq$ leads to a slightly higher R value for $RbCdF_3:Mn^{2+}$ than for $RbCaF_3:Mn^{2+}$ comes from the complex structure of the asymmetric $^6A_{1g}(S) \rightarrow {}^4A_{1g}(G)$, $^4E_g(G)$ band. In fact $10Dq$ is essentially determined by the difference $\Delta = E_3 - E_1$ between the energies of the third ($^6A_{1g}(S) \rightarrow {}^4A_{1g}(G)$, $^4E_g(G)$) and first ($^6A_{1g}(S) \rightarrow {}^4T_{1g}(G)$) maxima. Nevertheless, problems appear in the interpretation of the third band maximum because (i) the two $^6A_{1g}(S) \rightarrow {}^4A_{1g}(G)$ and $^6A_{1g}(S) \rightarrow {}^4E_g(G)$ transitions are neither exactly coincident (they are separated by 100 cm^{-1} in both $KMgF_3:Mn^{2+}$ and $KZnF_3:Mn^{2+}$ [30]) nor display the same

oscillator strength, and (ii) the associated vibronic structure can change for different systems.

In general, the vibronic couplings responsible for both the electric dipole oscillator strength and the phonon sideband of the crystal field transitions may be influenced not only by changes in R but mainly by the type of cations out of the first coordination sphere. In this way, both the phonon frequency and the electron–phonon coupling associated with the vibronic sidebands of the $^6A_{1g}(S) \rightarrow {}^4A_{1g}(G)$ and $^6A_{1g}(S) \rightarrow {}^4E_g(G)$ transitions as well as of the $^6A_{1g}(S) \rightarrow {}^4T_{1g}(G)$ one are indeed rather different in $KMgF_3:Mn^{2+}$ and $KZnF_3:Mn^{2+}$. Experimental evidence of these facts can be found elsewhere [30, 31]. The $T = 1.7$ K high-resolution spectra around the $^4A_{1g}$, $^4E_g(G)$ in $KMgF_3:Mn^{2+}$ and $KZnF_3:Mn^{2+}$ show that the dipolar magnetic zero-phonon lines are shifted 100 cm^{-1} towards higher energies in $KMgF_3:Mn^{2+}$ [30] at variance with the RT situation in which the band maximum for $KMgF_3:Mn^{2+}$ lies only 10 cm^{-1} below the $KZnF_3:Mn^{2+}$ one [5]. This result, which cannot be explained on the basis of different values of R, clearly suggests that vibronic couplings play a crucial role in determining the bandshape and therefore the band maxima in such non-$10Dq$-dependent $^4A_{1g}$, $^4E_g(G)$ tansitions. Such an effect could also justify the anomalous dispersion of the $^4A_{1g}$, $^4E_g(G)$ maxima, E_3, observed along the fluoroperovskite series whose variation, as shown in table 2, cannot be understood simply by changes in the Mn^{2+}–F^- distance. Taking into account the measured value $\partial E_3/\partial R = -15$ cm^{-1} pm^{-1} for $RbMnF_3$ [32], E_3 should *increase* by ~ 120 cm^{-1} if R increases by ~ 8 pm. Though this increase reflects the trend followed by E_3, this mechanism is unable to explain its variation between successive crystals along the series. This is particularly puzzling on going from $RbCdF_3:Mn^{2+}$ to $RbCaF_3:Mn^{2+}$ and $CsCaF_3:Mn^{2+}$ where blue shifts of 185 and 135 cm^{-1} are actually observed instead of the 30 and 50 cm^{-1} that should be expected from their respective R values.

This analysis suggests that spectroscopic studies of the R dependence of E_3 should be performed on a given crystal using hydrostatic pressure techniques and not chemical pressures where the use of different host matrices affects not only R but also the vibronic couplings. This effect is however not so important for the $10Dq$ dependent $^6A_{1g}(S) \rightarrow {}^4T_{1g}(G)$ excitation band, E_1, whose R dependence, $\partial E_1/\partial R = 200$ cm^{-1} pm^{-1}, is one order of magnitude higher than that of E_3.

Owing to this, we have fitted the experimental position of $^6A_{1g}(S) \rightarrow {}^4T_{1g}(G)$ maxima corresponding to fluoroperovskites containing Mn^{2+} to the equation:

$$E_1 = a + bR. \tag{2}$$

The constants a and b have been determined using the values of E_1 and R corresponding to $KMnF_3$ and $RbMnF_3$ as well as those for $KZnF_3:Mn^{2+}$ and $RbCdF_3:Mn^{2+}$. In the latter cases the distance, R, was determined through EXAFS [1]. The best values of the constants a and b were found to be $a = 21875$ cm^{-1} and $b = 194.3$ cm^{-1} pm^{-1}. The actual Mn^{2+}–F^- distance obtained for the other fluoroperovskites ($CsCaF_3$, $RbCaF_3$ and $KMgF_3$) doped with Mn^{2+} is in fact close to that derived using the experimental $10Dq$ value. The difference, ΔR, between the R values for $RbCaF_3:Mn^{2+}$ and $RbCdF_3:Mn^{2+}$ becomes $\Delta R = (0.3 \pm 0.2)$ pm. This difference, although positive, appears to be a little smaller than $\Delta R = (1.8 \pm 1.2)$ pm derived from the experimental A_s values.

If we compare two systems such as for instance $CsCaF_3:Mn^{2+}$ and $RbCdF_3:Mn^{2+}$ it is clear from table 2 that $\Delta R < \Delta R_0$. To be more specific, in these cases it is found that $f \equiv \Delta R/\Delta R_0 \cong 0.35$. Thus, accepting the same f value in the comparison between $RbCaF_3:Mn^{2+}$ and $RbCdF_3:Mn^{2+}$, a difference $\Delta R \cong 1$ pm could be expected.

It is worth noting that as $10Dq$ for systems with MnF_6^{4-} units is measured mainly through the difference $\Delta = E_3 - E_1$, the dispersion of data for E_3 is also reflected in the $10Dq$ values. This situation could explain the slightly different R values obtained through equations (1) and (2). In the less favourable case of $CsCaF_3:Mn^{2+}$, this difference is 0.9 pm.

Let us now focus on phase transitions of $RbCaF_3$ detected using optical parameters of the Mn^{2+} probe. Interesting results are obtained plotting the experimental first-order moment, M_1, of the emission band associated with $RbCaF_3:Mn^{2+}$ and comparing it to the corresponding variation displayed by $CsCaF_3:Mn^{2+}$. Such results are given in figure 2. It can be seen that above 100 K the first moment M_1 undergoes in both cases a progressive increase upon heating. This increase as previously discussed [29] *partially* reflects the effects of thermal expansion giving rise to a decrement of $10Dq$ and thus an increase of the $^6A_{1g}(S) \rightarrow {}^4T_{1g}(G)$ energy. Nevertheless, at variance with what is observed in $CsCaF_3:Mn^{2+}$ where the host lattice does not undergo a phase transition below 300 K [20], a slight but sensible change in the slope of $M_1(T)$ is detected in $RbCaF_3:Mn^{2+}$. Therefore this anomaly can reasonably be related to the $O_h^1 \rightarrow D_{4h}^{18}$ structural phase transition experienced by the host lattice at 193 K. It is worth stressing however that the detection of such a phase transition through $M_1(T)$ requires a lot of measurements of M_1 in the 300–100 K range. In the present work M_1 has been measured for about 40 different temperatures in this range. As a result of the change of the slope at 193 K, the extrapolated value M_1 at 0 K (called $M_1(0)$) would be about 50 cm^{-1} smaller for the tetragonal phase than for the cubic one. This can be related to a slightly higher $10Dq$ value for the former than for the latter case. If $\delta E_{CT}(0) = R_C(0) - R_T(0)$, where $R_C(0)$ and $R_T(0)$ denote the extrapolated Mn^{2+}–F^- distances at 0 K for the cubic and the tetragonal phases, respectively, a value $\delta E_{CT}(0) \simeq 0.2$ pm is *estimated* using equation (2).

Upon lowering the temperature another anomaly is detected in the neighbourhood of 40 K (figure 2). Here M_1 experiences a small but abrupt blue shift of ~ 100 cm^{-1} which can in fact be related to the existence of another phase transition leading to a decrement of $10Dq$ upon cooling. Such a decrease would imply an *increase* of the average Mn^{2+}–F^- distance, R, equal to ~ 0.5 pm following equation (2), leading to a relative increase $\Delta R/R \simeq 0.2\%$. It is worth stressing now that the compound $KMnF_3$, apart from the $O_h^1 \rightarrow D_{4h}^{18}$ structural phase transition at $T_{c1} = 184$ K, experiences also the $D_{4h}^{18} \rightarrow D_{4h}^5$ phase transition at $T_{c2} = 81.5$ K. Dilatometric measurements [33] reveal that when this first-order transition takes place the length, L, of the sample undergoes an abrupt *increase*, $\Delta L/L$ being equal to 0.18%. This value is similar to that derived for the phase transition of $RbCaF_3$ at $T_{c2} \simeq 40$ K.

Figure 2 depicts the temperature dependence of the luminescence lifetime for both $CsCaF_3:Mn^{2+}$ and $RbCaF_3:Mn^{2+}$ crystals. The experimental values for $CsCaF_3:Mn^{2+}$ have been fitted to the equation

$$\tau = \tau_0 \tanh(\hbar\omega_u/2kT) \tag{3}$$

characteristic of phonon assisted electric dipole transitions. $\omega_u/2\pi$ is the effective

phonon frequency. It can be seen that the fitting is very good with the exception of the experimental points lying in the $T < 50$ K region. The origin of this discrepancy, also seen in Mn^{2+} doped $KMgF_3$ and $KZnF_3$ [31], is at present not understood. In the case of $RbCaF_3:Mn^{2+}$ a similar fitting of the experimental points in the 50–300 K range using equation (3) leads to a worse agreement. Nevertheless, this law is obeyed above 200 K in $RbCaF_3:Mn^{2+}$ (solid line in figure 2). The progressive deviation of the experimental points below this temperature is also related to the existence of the $O_h^1 \rightarrow D_{4h}^{18}$ structural phase transition even though this parameter is less sensitive than $M_1(T)$. Furthermore, the curve $\tau(T)$ does not provide any evidence on the existence of the phase transition at $T_{c2} = 40$ K which is however well observed through M_1. Though the origin of this different behaviour displayed by $M_1(T)$ and $\tau(T)$ with respect to the phase transitions of the host lattice is not well understood, it is worth noting that similar situations have been encountered for other materials containing Mn^{2+} [34, 35] or Cr^{3+} [36].

As a main conclusion, this work offers for the first time good evidence of two phase transitions in $RbCaF_3$ detected through an optical parameter of the Mn^{2+} probe. Also it provides a consistent view of the relation between optical and EPR parameters of Mn^{2+} in fluorides and the equilibrium Mn^{2+}–F^- distance, R. Further work devoted to clarifying the dependence of zero-phonon lines and Stokes shifts upon R for Mn^{2+} doped fluoroperovskites is now in progress.

Acknowledgments

The authors would like to thank Professor R Alcalá for kindly supplying us the $RbCaF_3:Mn^{2+}$ sample. This work has been supported by the CICYT under project MAT 90-0668.

References

[1] Leblé A 1982 *Thèse d'Etat* Université du Maine, Le Mans, France
[2] Barriuso M T and Moreno M 1984 *Phys. Rev.* B **29** 3623
[3] Barriuso M T and Moreno M 1984 *Chem. Phys. Lett.* **112** 165
[4] Rodríguez F and Moreno M 1986 *J. Chem. Phys.* **84** 692
[5] Rodríguez F, Moreno M, Tressaud A and Chaminade J P 1987 *Cryst. Latt. Defects Amorph. Mater.* **16** 221
[6] Barkyoumb J H and Mansour A N 1993 *Phys. Rev.* B **46** 8768
[7] Moreno M 1990 *J. Phys. Chem. Solids* **51** 835
[8] Rousseau J J, Leblé A and Fayet C J 1978 *J. Physique* **39** 1215
[9] Jeck R K and Krebs J J 1972 *Phys. Rev.* B **5** 1677
[10] Aoeki H, Arakawa M and Yosida T 1983 *J. Phys. Soc. Japan* **52** 2216
[11] Studzinski P and Spaeth J M 1986 *J. Phys. C: Solid State Phys.* **19** 6441
[12] Modine F A, Sonder E, Unruh W P, Finch C B and Westbrook R D 1974 *Phys. Rev.* B **10** 1623
[13] Bates J B, Major R W and Modine F A 1975 *Solid State Commun.* **17** 1347
[14] Kamitakahara W A and Rotter C A 1975 *Solid State Commun.* **17** 1350
[15] Ridou C, Rousseau M and Treund A 1977 *J. Phys. Lett.* **38** L359
[16] Sakata M, Hidaka M and Storey J S 1979 *Solid State Commun.* **32** 813
[17] Buzaré J Y, Fayet-Bonnel M and Fayet J C 1980 *J. Phys. C: Solid State Phys.* **13** 857
[18] Hidaka M, Maeda S and Storey J S 1985 *Phase Transitions* **5** 219
[19] Rousseau M, Gesland J Y, Julliard J, Nouet J, Zarembowitch J and Zarembowitch A 1975 *Phys. Rev.* B **12** 1579
[20] Ridou C 1979 *Thèse d'Etat* Université du Paris VI, France

[21] Rousseau J J 1977 *Thèse d'Etat* Université du Maine, Le Mans, France
[22] Villacampa B, Casas González J, Alcalá R and Alonso P J 1991 *J. Phys.: Condens. Matter* **3** 8281
[23] Marco de Lucas C and Rodríguez F 1990 *Rev. Sci. Instrum.* **61** 23
[24] Luaña V, Bermejo M, Flórez M, Recio J M and Pueyo L 1989 *J. Chem. Phys.* **90** 6409
[25] Sugano S, Tanabe Y and Kamimura H 1970 *Multiplets of Transition-Metal Ions in Crystals* (New York: Academic)
[26] Drickamer H G and Franck C W 1973 *Electronic Transitions and the High Pressure Chemistry and Physics of Solids* (London: Chapman and Hall)
[27] Moreno M, Barriuso M T and Aramburu J A 1992 *J. Phys.: Condens. Matter* **4** 9481
[28] Walsh W M, Jeener J and Bloembergen M 1965 *Phys. Rev.* **139** A1338
[29] Rodríguez F, Moreno M, Dance J M and Tressaud A 1989 *Solid State Commun.* **69** 67
[30] Ferguson J, Güdel H U, Krausz E R and Guggenheim H J 1974 *Mol. Phys.* **28** 879
[31] Rodríguez F, Riesen H and Güdel H U 1991 *J. Lumin.* **50** 101
[32] Solomon E I and McClure D S 1974 *Phys. Rev.* B **9** 4690
[33] Bartolomé J, Rojo J A, Navarro R, Gonzalez D, Ibarra M R and del Moral A 1983 *J. Magn. Magn. Mater.* **31–4** 1052
[34] Marco de Lucas M C and Rodríguez F 1989 *J. Phys.: Condens. Matter* **1** 4251
[35] Marco de Lucas M C, Rodríguez F and Moreno M 1990 *Ferroelectrics* **109** 21
[36] Marco de Lucas M C, Rodríguez F, Dance J M, Moreno M and Tressaud A 1991 *J. Lumin.* **48 & 49** 553
[37] Rodríguez F and Moreno M 1986 *J. Phys. C: Solid State Phys.* **19** L513